Gas Hydrate Formation

And Dissociation Numerical Modelling with Nitrogen and Carbon Dioxide

***Callum Smith**[curtin university]

Curtin University, 5 De Laeter Way, Bentley 6102, Perth WA. Australia

callum.c.smith@student.curtin.edu.au

Ahmed Barifcani[curtin university]

Curtin University, 5 De Laeter Way, Bentley 6102, Perth WA. Australia

a.barifcani@curtin.edu.au

David Pack[gas measurement & auditing pty ltd]

Gas Measurement & Auditing Pty Ltd, P.O Box 458.Kalamunda 6926, Perth WA. Australia

gasmeasurement@bigpond.com

***Corresponding Author**

Abstract

This work aims at providing experimental data for various methane-based hydrates, namely nitrogen and carbon dioxide gas mixtures with varying concentrations to provide an empirically based hydrate equilibrium model. Acquired using a sapphire pressure – volume – temperature (PVT) cell, this data is used as the foundation for the derivation of a model able to calculate the equilibrium temperature of a nitrogen and/or carbon dioxide diluted methane gas is accomplished. There are several theoretical predictive models used in software which can provide hydrate formation and equilibrium data, however theoretical models appear to outnumber experimental data and empirical models for which a comparison can be made. The effect of nitrogen and carbon dioxide, an inhibitor and promotor respectively, on methane hydrate formation and dissociation and their associated pressure and temperature conditions are explored. The hydrate profiles for various gas mixtures containing the gases mentioned are presented at pressures ranging between 40-180 bara. These hydrate profiles and the model presented were compared to those predicted by hydrate computational software and experimental data from other studies for verification. The derived model proved to be reliable when applied to various gas mixtures at different pressure conditions and was consistent when compared to computational software based on theoretical models. Consistency of methane hydrate formation data was compared to dissociation data proved that the formation temperature is not an accurate representation of the equilibrium temperature. A simple statistical measure revealed the dissociation temperature measurements to be more precise and agreed to a much larger degree with literature.

Keywords: Gas hydrate, numerical model, methane, nitrogen, carbon dioxide

1.0 Introduction and Background

Natural gas hydrates are crystalline solids composed of water and gas which occur in nature at high pressure and low temperature conditions (E. D. Sloan 2008). The water (host) forms hydrogen bonded cavities which surround and enclathrate the gas (guest) molecule to form a crystalline solid resembling ice. Depending primarily on the size of the gas molecule, three different common gas hydrate structure types exist; structure I (sI), structure II (sII) and more recently structure H (sH). Smaller molecules such as methane, ethane and carbon dioxide typically form sI hydrates which are the most abundantly occurring hydrate structure in nature, with a preference to methane gas hydrates (Schicks 2010). Natural gas hydrates continue to be a significant issue in oil and gas recovery and processing because of their ability to form in convenient operating conditions. High pressure and low temperature are

ideal conditions for gas hydrate formation, however several other factors contribute to hydrate formation and the nature of their formation. In terms of stability, gas molecules are required to be small enough to fit inside the water cavities but also be large enough to provide stability to the hydrate structure (Buffet 2000). A guest molecule approximately 75% the size of the cavity is required to provide adequate structural stability of the resultant hydrate whereas if the molecule is over 100% the size of the cavity, the structure cannot stabilize and the hydrate will not form. A similar situation arises if the gas molecule size is significantly less than 75% of the cavity. In this case, the gas molecule is not large enough to supply adequate stability therefore preventing formation from occurring (Christiansen and Sloan 1994). This has given rise to a significant amount of research in this field to combat the threats to productivity caused by gas hydrates.

Literature and experimental data informs us of nitrogen and carbon dioxide hydrate profiles but less of it is concerned with the effect these gases have on the hydrate profile of methane gas or natural gas for that matter, with methane being the primary component of natural gas. Detailed in this article are hydrate profiles explaining and illustrating the effect these gases have on methane gas from a hydrate perspective via experimental data collected using a sapphire microcell. This study uses this information to construct an empirical model describing these equilibrium conditions. Additionally, this data is compared to computational software, namely Aspen HYSYS and Calsep PVTsim, to aid in the comparison between experimental and theoretical hydrate data and to confirm the reliability of the derived numerical model. The hydrate conditions predicted by these programs and their modes of calculation are investigated by inspecting the method, sources of necessary parameters such as critical properties and Langmuir constants associated with the equations of state (EOS) and hydrate equilibrium computations performed respectively. Each is compared to make a judgement on the cause of variation between predictions based on two equations of state, Peng-Robinson (PR) and Soave-Redlich-Kwong (SRK). In addition, experimental data from other works such as Jhaveri and Robinson (1965) and Adisasmito et al. (1991) are portrayed to illustrate the likeness to the model presented as well as any disagreement.

1.1 Empirical Model Derivation

Using experimental data, a relationship between the hydrate dissociation conditions of a methane-nitrogen-carbon dioxide gas has been developed. This has been achieved by deriving a constant based on how much the inclusion of nitrogen and carbon dioxide influence the dissociation temperature in a methane-based gas. The dissociation temperature of a gas mixture containing methane, nitrogen and/or carbon dioxide is

empirically derived using the exponential equations that best describe the experimental nitrogen and carbon dioxide data.

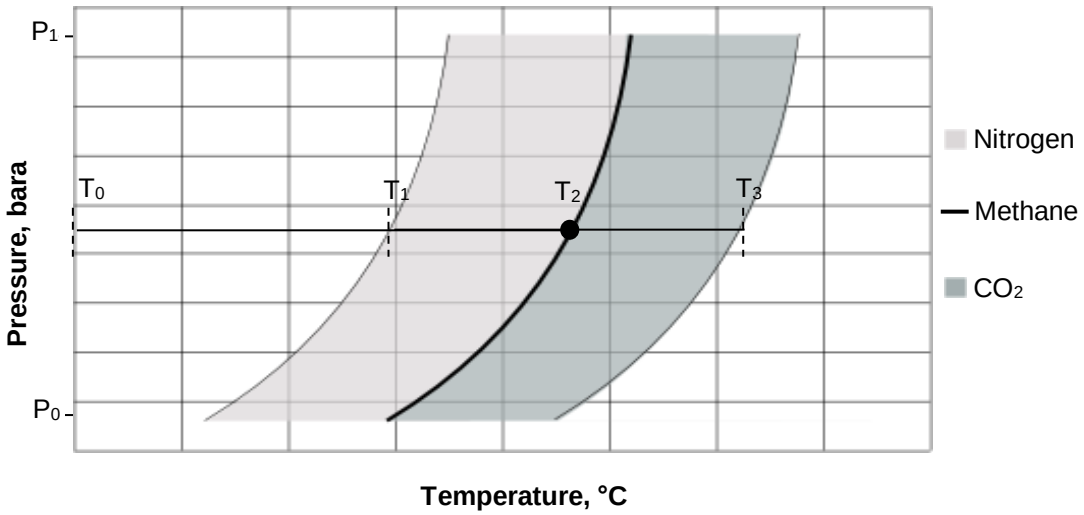

Fig.1 – Methane Hydrate Profile Shift

The deviation from the methane reference due to nitrogen and carbon dioxide (**Fig.1**), is summed by integrating between the appropriate pressure interval, P_1-P_0. These are denoted $\int_{P_0}^{P_1}(T_1\text{-}T_0)dT$ for nitrogen and $\int_{P_0}^{P_1}(T_3\text{-}T_0)dT$ for carbon dioxide. These quantities are compared to pure methane, $\int_{P_0}^{P_1}(T_2\text{-}T_0)dT$, in the form of a ratio, $\frac{\int_{P_0}^{P_1} T_1\text{-}T_0}{\int_{P_0}^{P_1} T_2\text{-}T_0}$ for nitrogen and $\frac{\int_{P_0}^{P_1} T_3\text{-}T_0}{\int_{P_0}^{P_1} T_2\text{-}T_0}$ for carbon dioxide. The dissociation temperature, T_d, is empirically expressed as,

$$T_d(P,x_{N2},x_{CO2}) = T_2(P) + \ln(P/a_{N2})\frac{x_{N2}}{x_{N2,ref}b_{N2}}\left(\frac{\int_{P_0}^{P_1}(T_1\text{-}T_0)dT}{\int_{P_0}^{P_1}(T_2\text{-}T_0)dT} - \frac{\int_{P_0}^{P_1}(T_2\text{-}T_0)dT}{\int_{P_0}^{P_1}(T_2\text{-}T_0)dT}\right)\ldots$$

$$\ldots + \ln(P/a_{CO2})\frac{x_{CO2}}{x_{CO2,ref}b_{CO2}}\left(\frac{\int_{P_0}^{P_1}(T_3\text{-}T_0)dT}{\int_{P_0}^{P_1}(T_2\text{-}T_0)dT} - \frac{\int_{P_0}^{P_1}(T_2\text{-}T_0)dT}{\int_{P_0}^{P_1}(T_2\text{-}T_0)dT}\right)\ldots\ldots\ldots \text{Eq. 1}$$

Symbols have their usual meaning; P and T are pressure and temperature respectively, x_{N2} is the nitrogen mole fraction, x_{CO2} is the carbon-dioxide mole fraction, a and b are constants from the exponential relation and $x_{CO2,ref}$ and $x_{N2,ref}$ are the mole fractions of the experimental gases used to generate data. Generating experimental hydrate profiles allows the areas

between the equilibrium lines to be evaluated. The model is not dependent on the volume of water present on the basis that the water volume is small and is insignificant compared to the moles of gas in each hydrate experiment. This is shown later on to be true (section 4.32); the resultant model is presented in section 4.5.

2.0 Methodology

2.1 Introduction

The primary apparatus used for the research work was a sapphire cell and an associated flow loop housed at the Clean Gas Technologies Australia (CGTA) laboratory. CGTA specialises in hydrate technology and carbon dioxide capture. The simplistic flow loop was designed to be as accessible as possible predominantly because of the use of manual ball valves. All tubing used in the flow loop is 1/4 inch with all fittings.

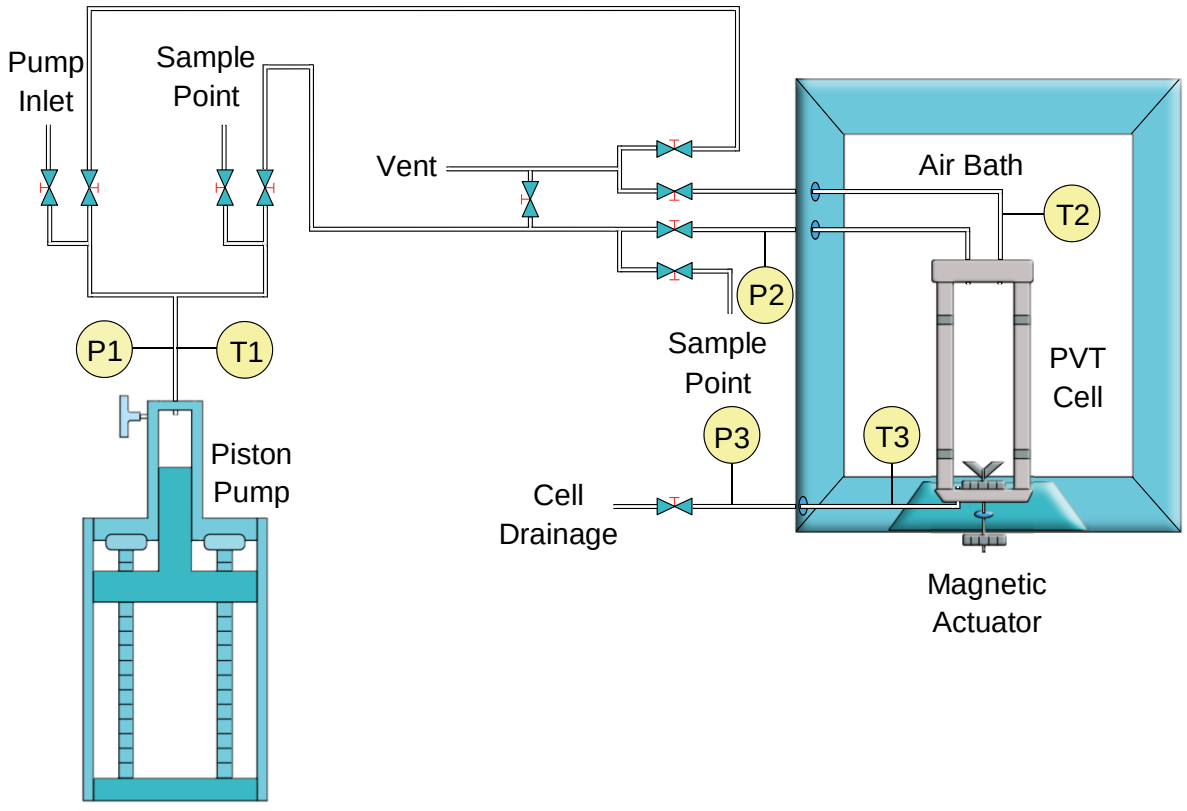

Fig. 2 – Sapphire Cell Schematic

The PVT cell (**Fig. 2**) is capable of enduring pressures in the vicinity of 500 bara and temperatures down to -160 °C when liquid nitrogen is used as the coolant, however cooling water is sufficient. For the purpose of this work, the PVT cell was operated in the ranges of 40-180 bara and 0-30 °C. The volume of the cell is 80 cm^3 non-inclusive of internal tubing;

this cannot be ignored because the volume of gas in the tubing is 25.8 cm^3 based on its 74 cm length and 1/4 in diameter. This equates to a total volume of 105.8 cm^3. The cell is protected by thick glass allowing it to experience high pressures and is separated from the outside environment by a reinforced and insulated door. Six clamps attached to the door allow for a tight seal, minimizing heat transfer through the housing of the PVT cell.

2.2 Application of Apparatus

A piston pump is implemented for the pressurization of gas and is maintained via software that controls the position of the piston. Pressure is monitored by pressure sensors and controlled via a Baldor motion PID controller which is linked with Mint Workbench software for inputting pressure set points and monitoring. This software also controls the temperature of the cell. To provide constant temperature monitoring of the gas and liquid phase, a thermocouple is secured at the top and bottom of the cell. The temperature of the water is the control temperature which however affects the gas temperature. Temperature increments are therefore small in order to ensure there is a minute temperature differential between each phase. A computer interface used in conjunction with FALCON software allows the set temperature to be input manually and is maintained with the proportional-integral-derivative (PID) controller associated with the software. The cooling is supplied by a chiller and for heating, the PVT cell uses an electrical heater. Cooling and heating is amplified by the use of a fan which circulates the heated or cooled air throughout the air bath chamber.

The process is fitted with sample points, allowing the gas to be analysed to confirm its composition. For venting and purging, an additional line is connected to the cell in which gas is safely vented through an outlet to the roof of the building and released to the atmosphere. Finally, the magnetic stirrer provides adequate mixing and promotes hydrate formation; it is controlled manually with a dial for changing the rotational velocity. The stirrer measures 2 inches across and is maintained at approximately 120 revolutions per minute (RPM) through each experimental procedure. This stirrer is essential because it disturbs the surface of the water. Without this disturbance, hydrates form only at the surface similar to a sheet of ice which blocks further dissolving of gas molecules, therefore halting further hydrate formation. This effect is observed when excess water was placed into the cell which adequately covered the top of the mixer and resulted in the mixer being unable to sufficiently mix the top region of water.

2.3 Apparatus Operating Requirements

The temperature search method is employed as the technique used to determine the hydrate formation and dissociation temperature of the nitrogen and carbon dioxide diluted methane gas mixtures. This involved stimulation in the form of cooling and heating of the PVT cell contents to promote hydrate formation and dissociation respectively. Temperature control of the cell contents is an important aspect of the procedure because the point of hydrate formation and dissociation is dependent on temperature. Changing the temperature of the cell too quickly can result in skipping the observable moment of formation or dissociation, giving biased results. For this reason, heating and cooling is used cautiously to counteract the possibility of this occurrence.

2.4 Gas Preparation

Gas mixture preparation involved pressurizing individual gas canisters with methane gas and the diluting gas, usually one or two of each depending on the pressure requirements of the experiment. Initially, the canisters are vacuumed and weighed with an electronic balance (linearity $\pm$ 0.02g) and then pressurized. They are then weighed again and the difference calculated. This is converted into moles and the mol% is calculated. Gas is released from the cylinder containing the excess gas or another canister is pressurized with the limiting gas and the process is repeated until the molar ratios are correct. The methane, nitrogen and carbon dioxide gas are all supplied by BOC Australia and are of high purity grade (99.99%) and distilled water is used for the water in the cell. To analyse the gas composition of prepared gas mixtures, an MSR Electronics methane composition analyser is used. Because only bi-component mixtures are used, all of which include methane, the remaining gas composition is easily determined.

2.5 Experimental Procedures

Prior to operation, the PVT cell, piston pump and flow loop are purged with nitrogen to relieve the plant's internals of any foreign species that may affect results. The remaining gas is vacuumed and the gas canisters are connected to the manifold and their contents released into the piston pump. Distilled water (5 mL) is syringed into the PVT cell through an opening on the steel palette connecting the tubing to the cell chamber. The gas is pressurized into the cell and allowed to thermally equilibrate before reducing the temperature. A temperature close to, but within a safe distance of the formation temperature is approached, which is estimated based on previous results and computational software. The cooling rate is slowed significantly to approximately 2 °C per hour until hydrate formation is clearly observed. Temperature is maintained until hydrate formation and crystallization is complete. The hydrate solid is then heated to a temperature within range of

the dissociation temperature and the heating rate reduced to 2 °C per hour when the dissociation point is approached. Hydrates are allowed to fully dissociate while maintaining a 2 °C per hour heating rate. Finally, the apparatus is emptied of its contents and cleaned for future experimental processes.

3.0 Macroscopic Observations

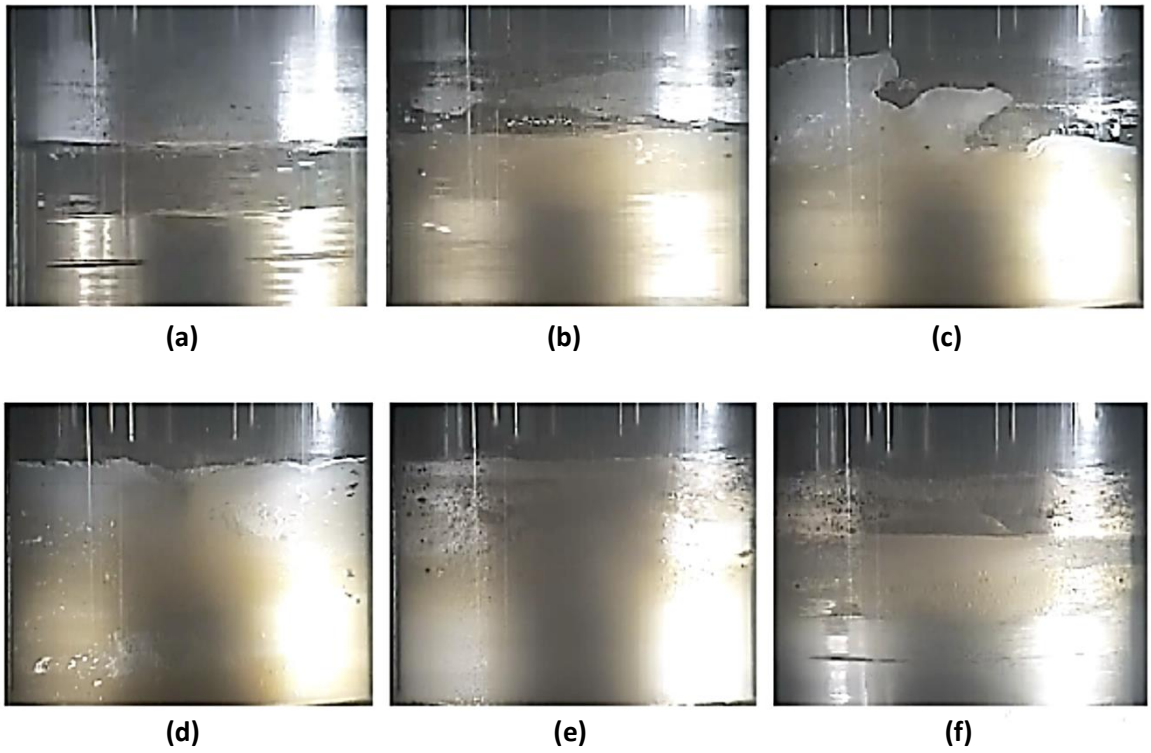

Fig.3 – (a) Initial Formation (b) Late Formation (c) Hydrate Growth (d) Crystallization (e) Initial Dissociation (f) Late Dissociation

After an adequate degree of sub-cooling, usually 2-4 °C below the dissociation temperature, unstable agglomerates formed upon the initial dissolving of gas molecules formed more stable structures. These reached a critical size and formed observable nuclei, giving the mixture an appearance akin to that of **Fig.3 (a)**. This initial formation of hydrate solids occurred at the interface of the liquid and gas phases. These observations are supported in the works of Mori (1998) who performed a study and review of the characterization of hydrate films where he also makes notes regarding hydrate formation initializing at the interface. When allowed to progress, the mixture further developed into a more hydrate-concentrated state, closely resembling crushed ice mixed with water **(b)**. The mixture was still very capable of flowing at this stage with very little observed resistance which was

inferred from the ease of the actuator maintaining a constant rotational velocity. Hydrates initially formed quite rapidly in which the rate of formation appeared to decrease over time. This is explained by the reduced concentration difference between the solution and hydrates; consequently the rate of formation reduces when the temperature is not changed. As the contents transitioned to a crystallized state **(d)**, the hydrate solids developed from small solids to significantly larger solids **(c)** from further nucleation and growth. The formation of these particular hydrate solids appeared to have little effect on the flow of the mixture; however as larger sized hydrates developed, a noticeable decline in flow of the mixture occurred. Consequently, the magnetic actuator struggled to maintain its normal rotational velocity and often slipped. This phenomenon occurred more frequently and to a greater extent as these solids further increased in size. The large hydrates eventually increased to a very large size until the liquid phase was nearly consumed and crystallized to form a continuous solid hydrate phase **(d)**. Because of the reduced liquid medium, the contents are completely immovable by the magnetic actuator. Under thermal stimulation of the crystallized solid, dissociation subtly occurred and was sometimes difficult to notice because of the slow rate of heating. It was detected by small cavities that appeared in the hydrate phase **(e)** and was accompanied by a wet film. Under continued stimulation, the structure decomposed from a single hydrate structure into fragments. This was accompanied by simultaneous liquid formation which pooled at the bottom of the cell and enabled the actuator to mobilize, although this mobilization was severely hampered by the large fragments. Throughout the dissociation phase of the experiment, liquid formation was very evident on the outside of the cylindrical hydrate structure caused by the radial dissociation. The hydrate mixture flowed more easily as more liquid was produced and resulted in reduced hydrate radii and concentration of the dissociating hydrate fragments. Hydrate dissociation continued to reform the liquid and liberate gas from its hydrate state until the hydrate solids were greatly diminished in size **(f).** Dirt is also commonly deposited on the inside of the cell during dissociation and adheres to the glass and this outlines the importance of purging and vacuuming which when not performed produces significantly more dirt than illustrated (f). The mixture, now in a comparable state to (b), was able to flow freely without any perceived significant resistance offered by the small hydrates still present. The remaining hydrates were easily dissociated at which point no hydrate phase was observed and the liquid and gas phases appeared to be completely restored.

4.0 Results and Discussion

It is well understood in the oil and gas industry that gas hydrates have a tendency to occur at high pressure and low temperature conditions. This is well documented through the works of

Sloan, Ripmeester and many others and is confirmed by the hydrate profiles constructed in this study. As a reference, the hydrate profile for pure methane was established with experimental data so that the hydrate data for nitrogen and carbon dioxide diluted methane mixtures can be compared.

4.1 Equilibrium Results

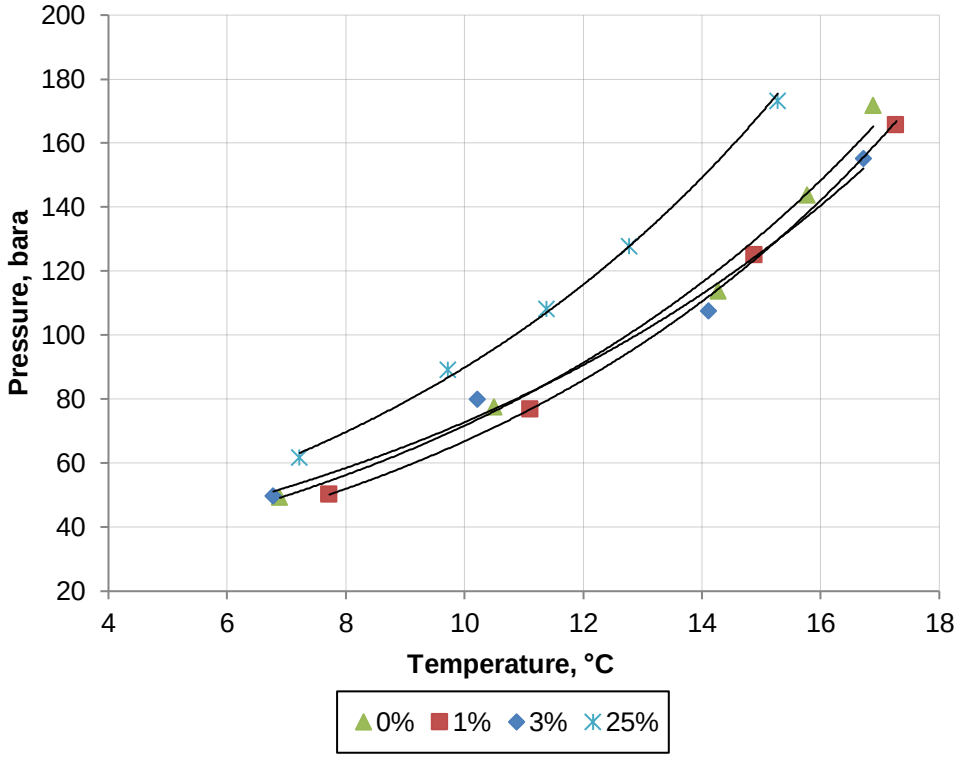

Fig.4 – Dissociation Temperature Profile for Nitrogen in Methane

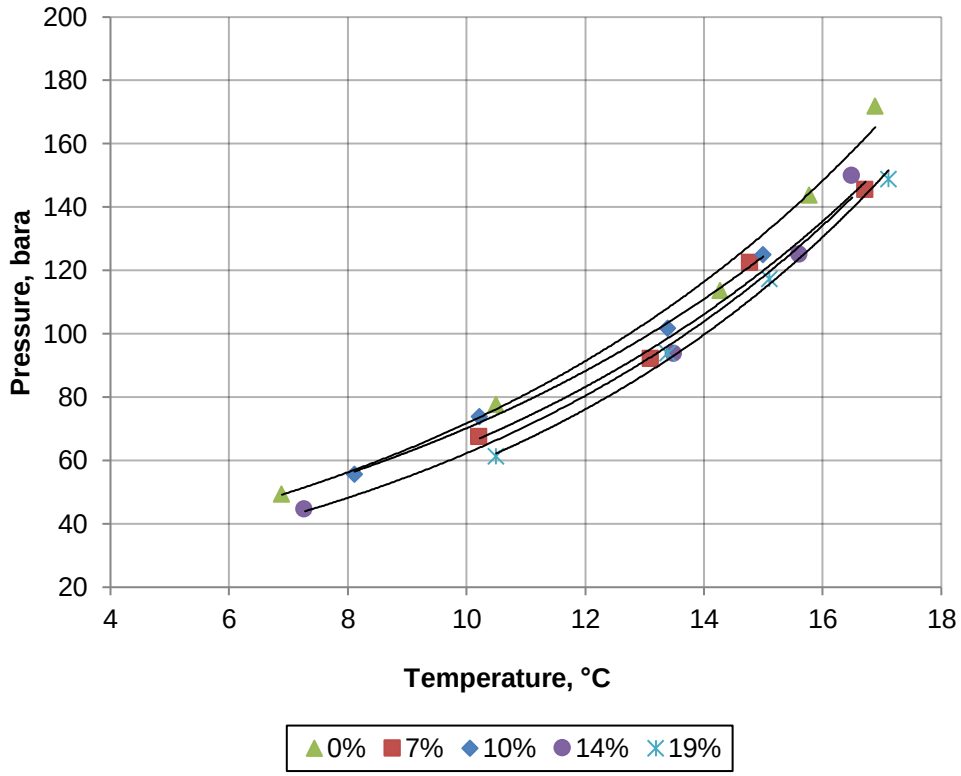

Fig.5 – Dissociation Temperature Profile for Carbon Dioxide in Methane

A noticeable decrease in equilibrium temperature occurs when nitrogen is introduced to methane gas**.** The hydrate equilibrium pressure for pure nitrogen is in excess of 200 bara at the lowest temperature settings in this study; this effectively renders the nitrogen hydrate-inert. Nitrogen is acting as a diluent, reducing the methane composition and therefore depressing its hydrate equilibrium conditions. The addition of 1 and 3 mol% of nitrogen is a very small dilution and results in significant overlap of their respective hydrate dissociation conditions. A very noticeable reduction in dissociation temperature with 25% nitrogen occurs as a result of significant dilution and reduction of methane partial pressure. As the nitrogen content is increased, a lower composition of methane exists in the liquid phase and therefore resulting in the reduction of the equilibrium temperature (ZareNezhad et al. 2015). Contrary to nitrogen hydrates, carbon dioxide hydrates form and dissociate at higher temperatures. One similarity is that the composition directly influences its effect on the hydrate dissociation temperature (**Fig.5**). This is explained by several factors, one of which is carbon dioxide's higher solubility in water than methane. Therefore, a gas with a higher solubility will likely have a greater driving force for hydrate formation resulting in a higher equilibrium temperature. Additionally, carbon dioxide is a larger molecule than both methane and nitrogen and offers more stability to its hydrate structure Lederhos et al. (1993). Carbon-dioxide is more capable of filling and providing stability to the larger $5^{12}6^2$ cavities making methane-carbon-dioxide hydrate dissociation more energy intensive, and therefore requiring

a higher temperature. These observations are similar to those made by Herri, et al. (2011) whom performed experimental studies on similar gas mixtures. Although Raman Spectroscopy and x-ray diffraction are the most accurate procedures when determining the hydrate structure, use of the Clausius – Clapeyron equation can also be an effective estimate (Juan, et al. 2015). This method confirmed the hydrate structure types that formed in the hydrate experiments and is performed according to the equation,

$$\frac{d\ln(P)}{d(1/T)} = \frac{\Delta H}{ZR} \quad \text{. . . . . Eq. 2}$$

Using the dissociation conditions represented in previous figures, the data is easily manipulated to be expressed as the Clausius – Clapeyron equation (**Eq. 2**) in graphical form.

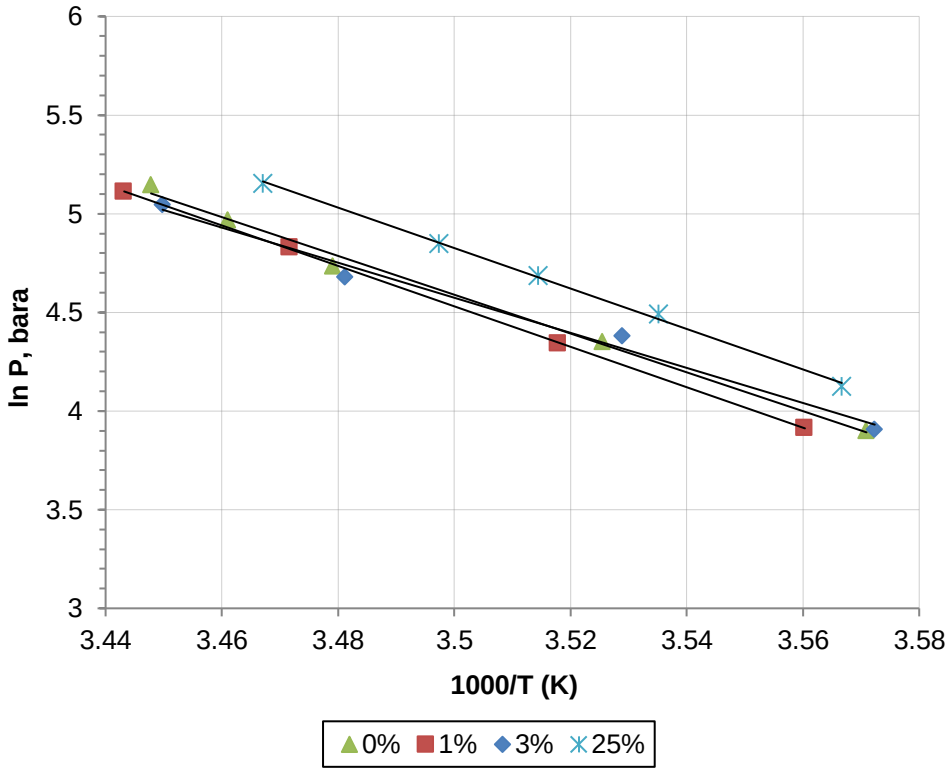

Fig.6 – Clausius-Clapeyron Plot for Nitrogen in Methane

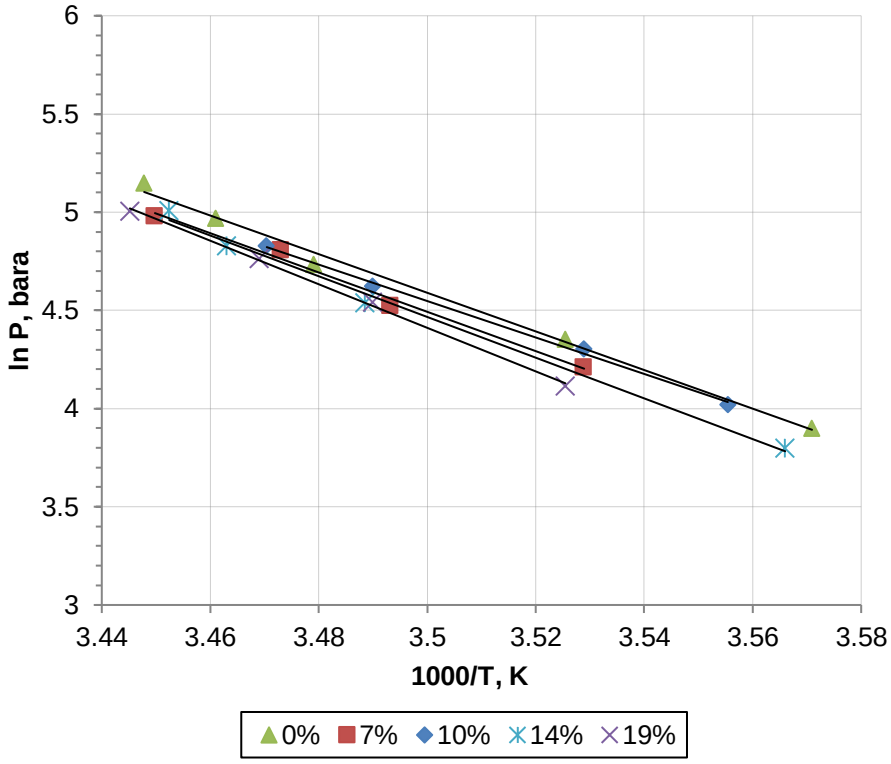

Fig.7 – Clausius-Clapeyron Plot for Carbon-dioxide in Methane

Slopes in the ranges of approximately -8900 to -10250 were calculated for methane-nitrogen hydrates and -9280 to -11100 for methane-carbon-dioxide hydrates. These are typical values for sI hydrates which are often in the range for sI hydrates (Sloan and Fleyfel 1992). This is expected to be the case simply by observing the plots in **Fig.6** and **Fig.7**. Both illustrations show only small deviations in the slope and therefore the hydrate structure is consistent in each hydrate profile. This is also an indication that no sII forming contaminant was present. Sloan (2008) also presented theoretical values for various gases. An equilibrium pressure and temperature of 177 bara and 17.5 °C respectively is detailed for methane. Interestingly, for nitrogen at a similar pressure of 160 bara, the corresponding temperature is 3 °C, confirming the dilution effect of nitrogen (**Fig.4**). An equilibrium pressure and temperature of 45 bara and 10 °C respectively are presented for pure carbon dioxide and for methane at a similar pressure value of 43 bara, a temperature of 5 °C is given. The increased hydrate temperature determined experimentally is supported by the trend observed in these literature values.

4.2 Formation Vs Dissociation

Each experimental point in the presented hydrate profiles throughout represents one data point. Ideally, three to four points would better represent each point in order to capture any variation which may be caused by experimental and human errors. Consequently, a test was

conducted for the purpose of determining the repeatability of methane hydrate formation and dissociation experimental data. This was an isobaric experiment at 100 bara and was performed four times for both the formation and dissociation temperature. The variation between results is calculated in the form of the standard deviation (**Table 1**) and variation is clearly observable in the methane hydrate profiles in **Fig.8**.

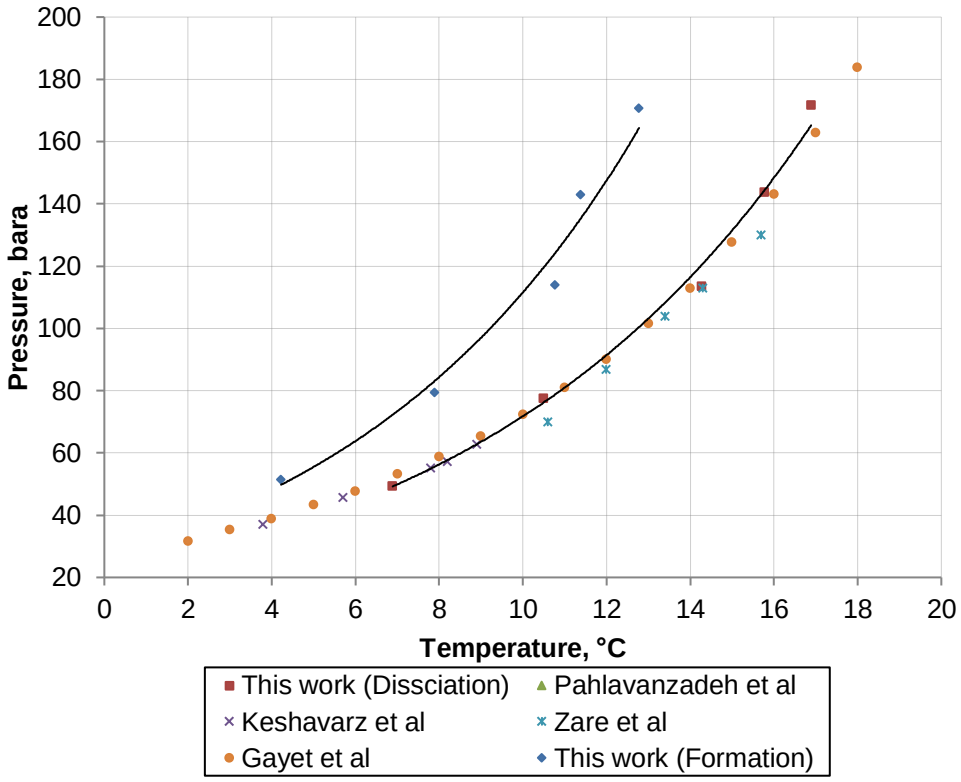

Fig.8 – Methane Hydrate Equilibrium Data; solid lines represent best fits of experimental formation and dissociation conditions

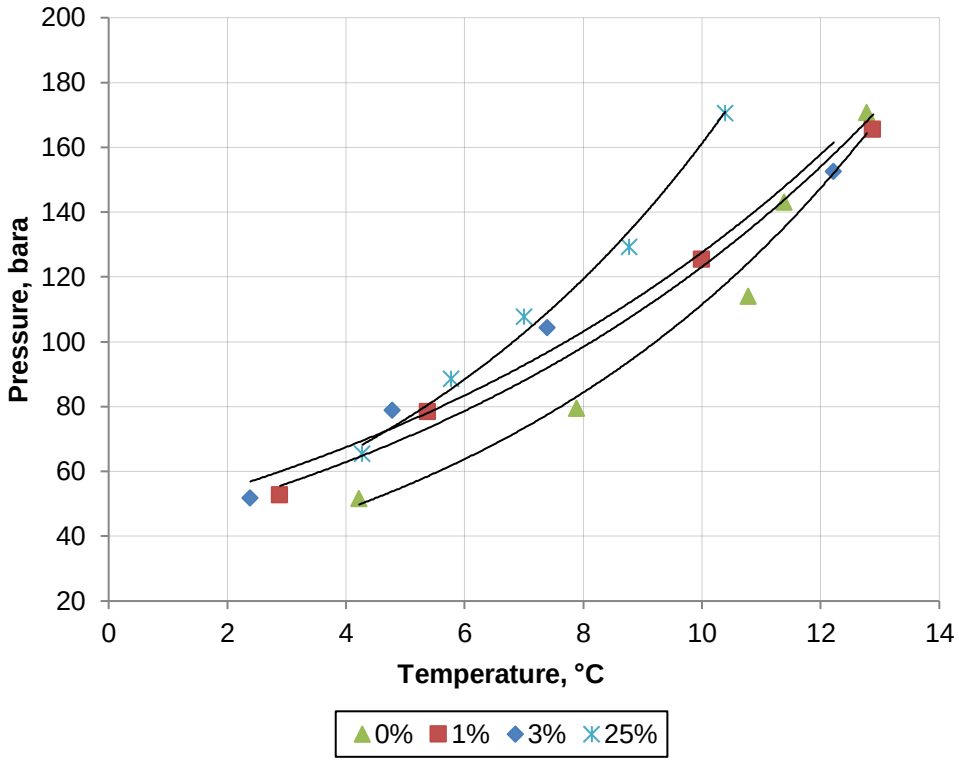

Fig.9 – Formation Temperature Profile for Nitrogen in Methane

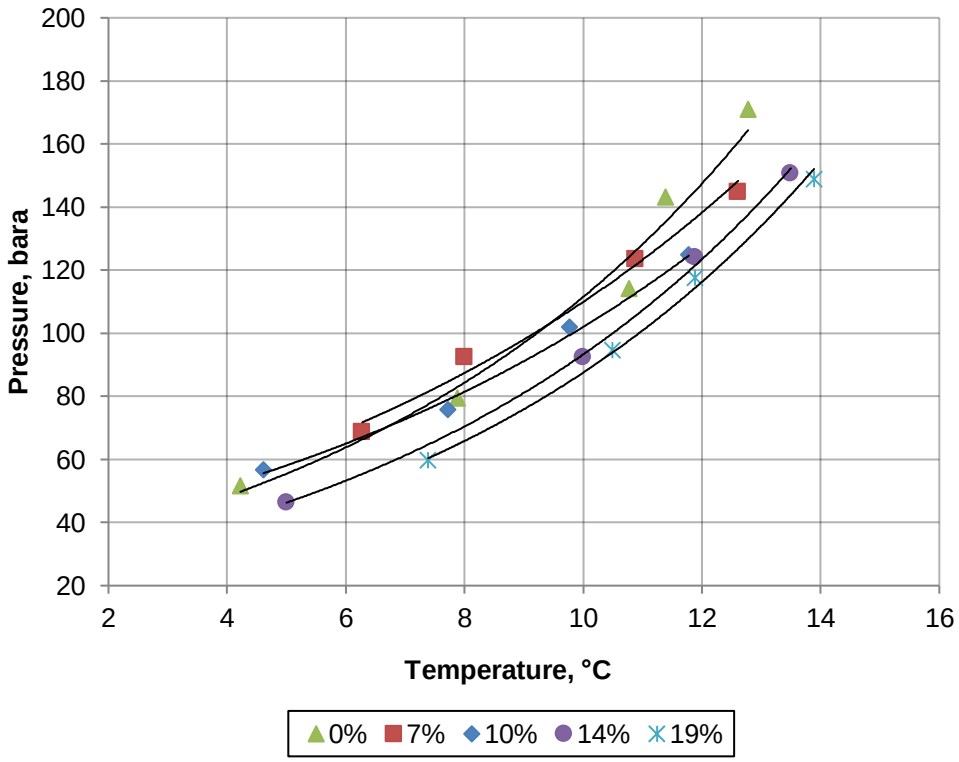

Fig.10 – Formation Temperature Profile for Carbon Dioxide in Methane

Table 1 – Methane at 100 bara

	TEST					
	1	2	3	4	Average	St. Dev
Formation (°C)	10.6	10.4	9.9	10.2	10.3	0.30
Dissociation (°C)	13.0	13.2	13.0	12.9	13.0	0.13

The formation temperature shows a much larger degree of variance compared to the dissociation temperatures due to its slight unpredictability arising from the large amount of factors affecting hydrate formation. On the contrary, the dissociation temperatures are consistent, only differing by a maximum of 0.3 °C. Because the dissociation temperature is essentially the equilibrium temperature and therefore is a fixed thermodynamic property (Tohidi, et al. 2000), this consistency is understandable. Contrarily, the formation temperature shows significantly more variation amongst the recorded data. Hydrate formation has a somewhat random nature to it, relying upon many factors but primarily the driving force for hydrate formation, $\Delta\mu$,

$$\Delta\mu = \sum_i n_i (T_l, P, x)\mu_{si}(T_l, P, x) + n_w\mu_w(T_g, P, x) - n_h\mu_h(P,T_l, z) \quad \text{Eq. 3}$$

In **Eq. 3** (Kashchiev and Firoozabadi 2002) n_i is the number of gas molecules in a hydrate unit cell with n_w water molecules, μ_{si} is the chemical potential of dissolved gas species i, μ_w is the chemical potential of water in solution, μ_h is the chemical potential of the hydrate phase, n_h is the number of moles of hydrate, T_g is the temperature of the gas, T_l is the temperature of the aqueous solution or hydrate and x and z are the mole fractions of the gases in the aqueous and hydrate phase respectively. A chemical potential driving force between the solution and the hydrate phase is required to initiate the formation of the first hydrate building blocks; it depends on the degree of sub-cooling, pressure and water content which in turn influence how quickly hydrates form after sub-cooling (Hobbs 1974). This has been shown by Christiansen and Sloan (1994) and in simulations (Ota and Qi 2000). The presence of impurities and the introduction of mechanical agitation stimulate formation and the nucleation rate reduce the degree of sub-cooling required for the time required for hydrate formation to induce (Dai et al. 2014). These factors can be controlled to a certain degree, but due to control limitations, conditions cannot be replicated exactly. Consequently, there is often noticeable variation in the experimental formation temperatures (**Fig.9 –**

Fig.10). The dissociation temperature is therefore better representative of the equilibrium point and is used synonymously throughout this paper.

4.3 Software Hydrate Predictions

4.31 HYSYS Prediction-Experimental Deviation

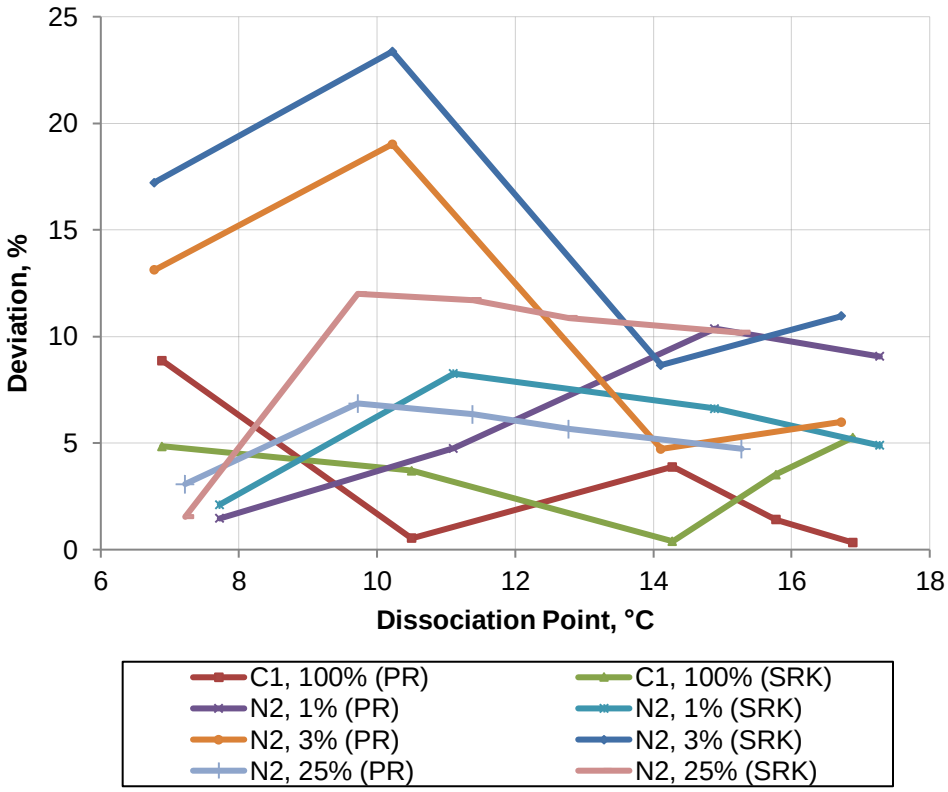

Fig.11 – N_2 HYSYS

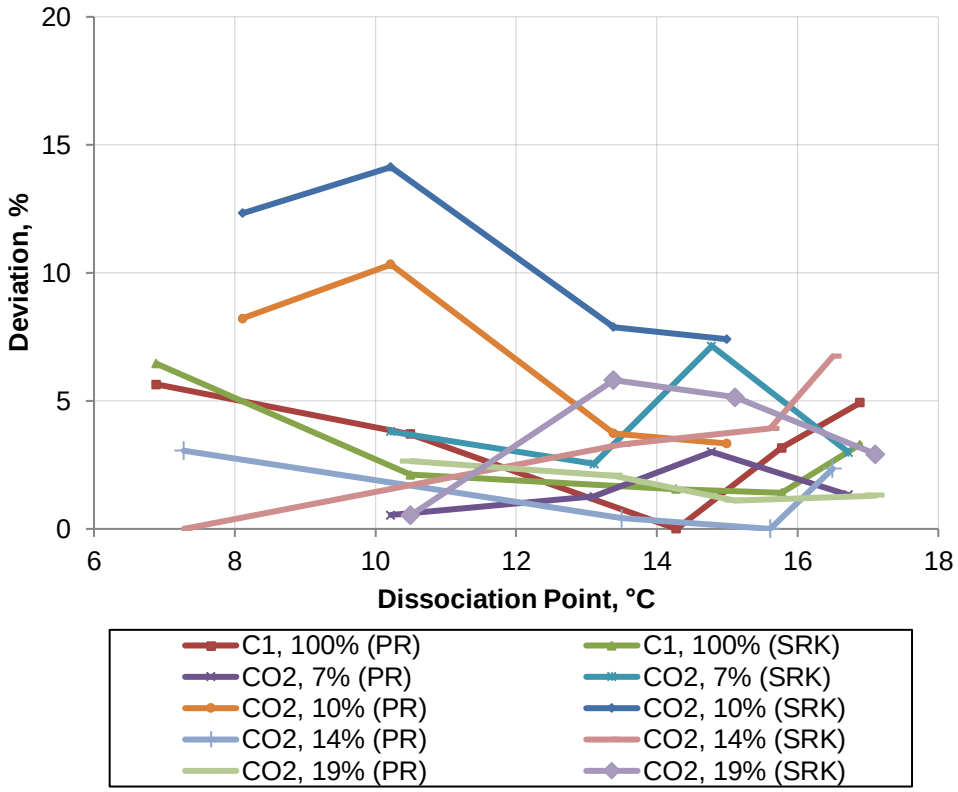

Fig.12 – CO_2 HYSYS

Utilising HYSYS's hydrate prediction software is relatively straight forward. A flow stream is simply created and specified with the correct composition, which is analysed by the hydrate utility using the fluid package/s chosen, PR and SRK in this case. Depending on the specified pressure, HYSYS then calculates the corresponding hydrate temperature based on the selected fluid package and another parameter detailed as the 'calculation mode'. Four different modes are available, namely 'Symmetric Model', 'Asymmetric Model', 'Vapour Only Model' and 'Assume Free Water'. In all mixtures tested, the calculation mode had a very negligible effect on the calculated hydrate temperature.

4.32 PVTsim Prediction-Experimental Deviations

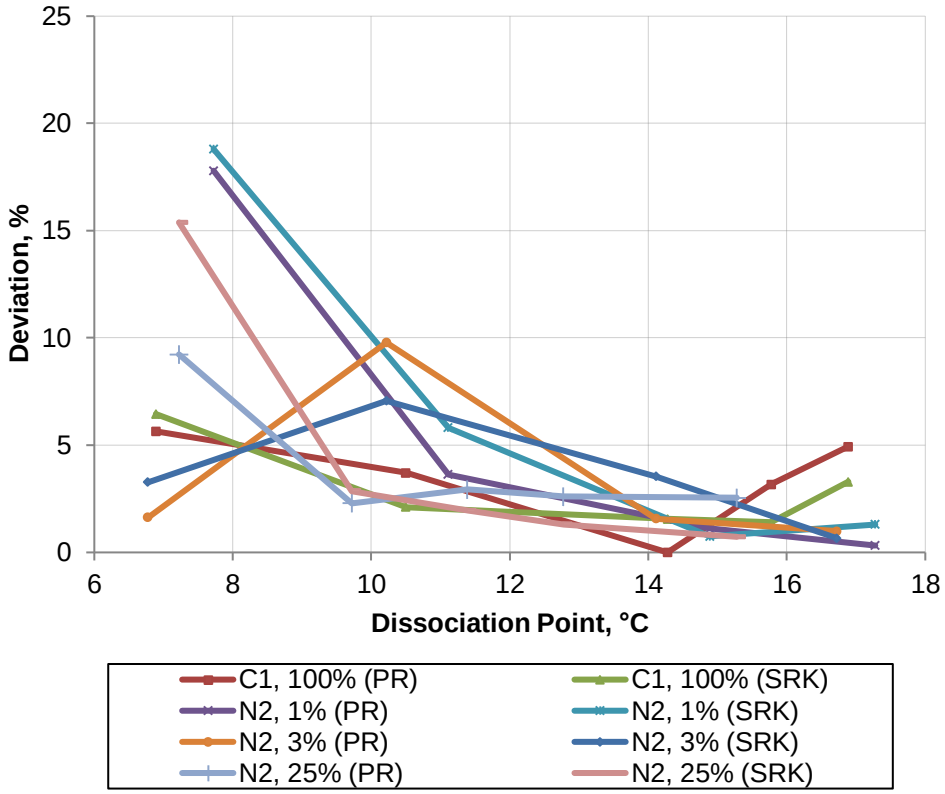

Fig.13 – N_2 PVTsim

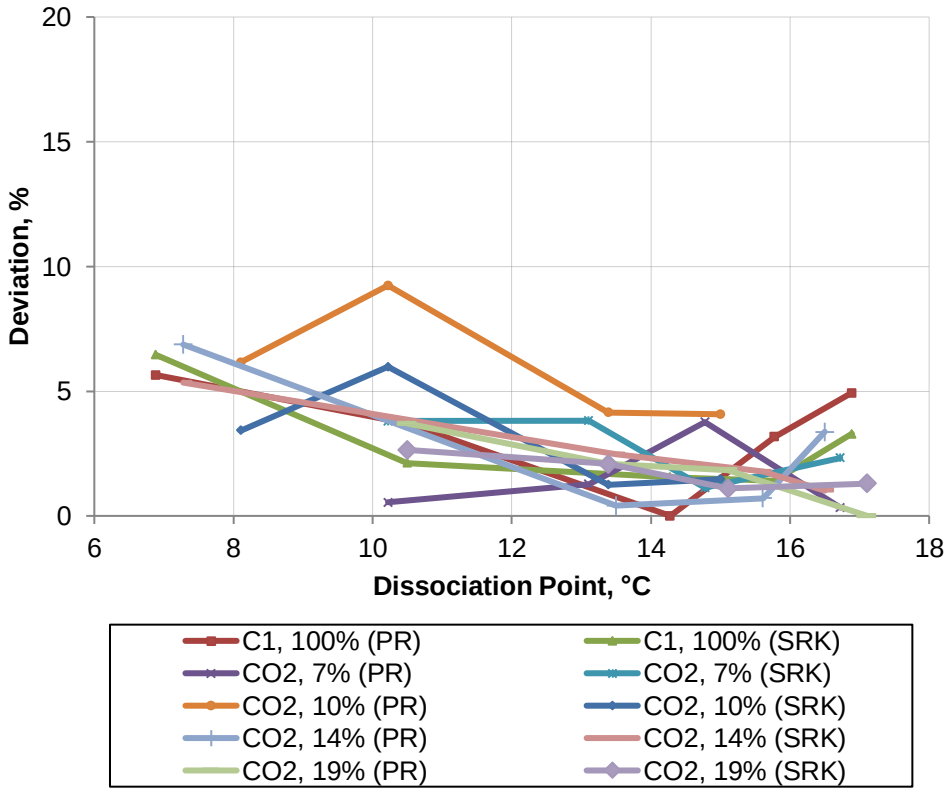

Fig.14 – CO_2 PVTsim

PVTsim operates differently than HYSYS in that it doesn't simulate chemical processes, but focuses on analysing almost any fluid from a PVT perspective with a major focus on petroleum fluids. Many different types of analyses are available ranging from phase diagrams, saturation point, viscosity, wax, asphaltene, and reservoir and hydrate analysis. The hydrate analysis only requires the composition of the gas mixture, which is input using PVTsim's fluid management tab and selecting an appropriate equation of state. Unlike HYSYS, PVTsim prompts for the amount of water present, which is input as the water/gas molar ratio. For all experiments, this ratio ranged between approximately 0.9 – 3.5 mol/mol and was determined by the following procedure,

1. Calculate number of water moles for the 5 mL of water; 0.277 mol
2. Calculate the number of gas moles for both the highest, 180 bara, and lowest pressures tested at, 50 bara; approximately 0.961 and 0.237 mol respectively using $n = \frac{PV}{ZRT}$ knowing the cell volume to be 105.8 cm^3
3. Evaluate the water/gas molar ratio at each pressure to provide the range, 0.86 – 3.47 mol/mol

The hydrate temperatures calculated at these molar ratios differed on a very small scale for each gas mixture, such that it was deemed negligible. Therefore the varying amounts of water introduced into the cell relative to the moles of gas clearly do not influence the equilibrium system significantly in this study.

4.4 Software Prediction Methods

There are many available software packages which have hydrate predictive capabilities. These programs primarily make use of various thermodynamic equations and correlations to provide an estimate of the conditions at which hydrates will form for a particular fluid. This study has made use of Aspen HYSYS and Calsep PVTsim, for the purpose of comparing experimental data from this work to the hydrate formation conditions calculated by these software packages. Recommended by HYSYS and PVTsim, the Peng-Robinson (PR) and Soave-Redlich-Kwong (SRK) fluid packages were used when utilising both programs. It is noted that versions 7.2 and 20 of HYSYS and PVTsim respectively were used when computing hydrate data. The hydrate data for pure methane, nitrogen and carbon-dioxide is presented for each model as a source of comparison between hydrate predictions for pure species and mixtures of these gases with methane (**Fig.15** – **Fig.17**).

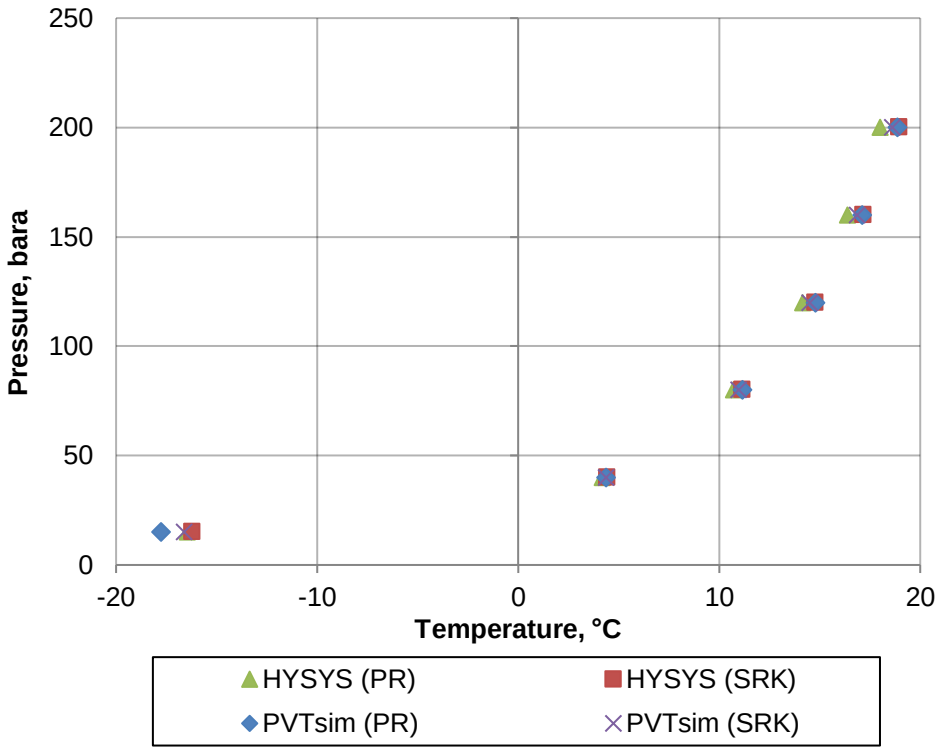

Fig.15 – Software Hydrate Equilibrium Data for Methane

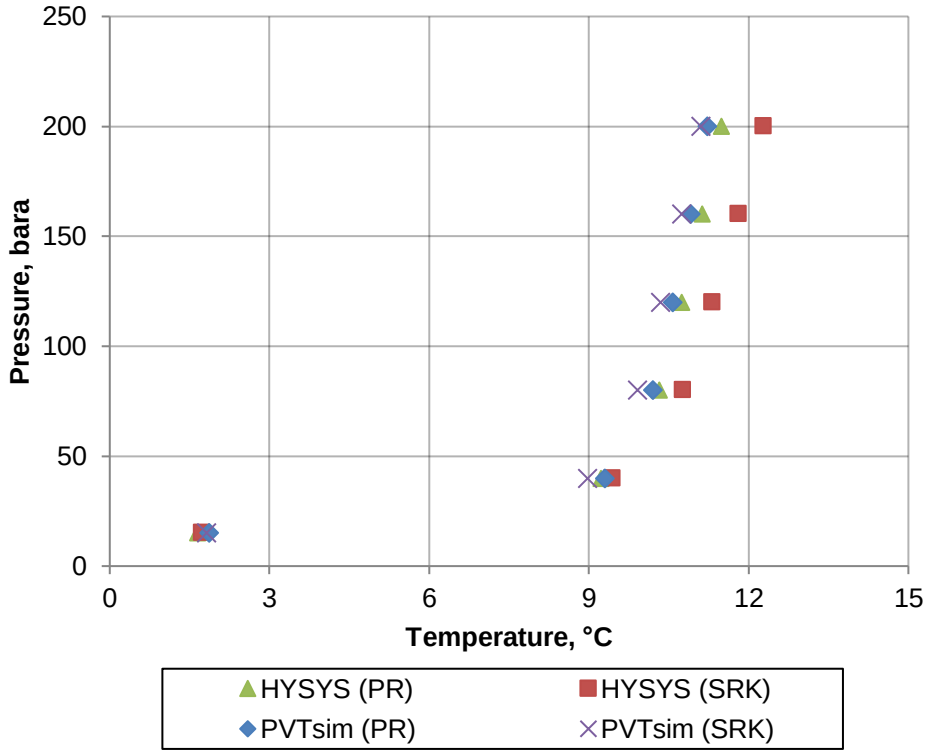

Fig.16 – Software Hydrate Equilibrium Data for Carbon-dioxide

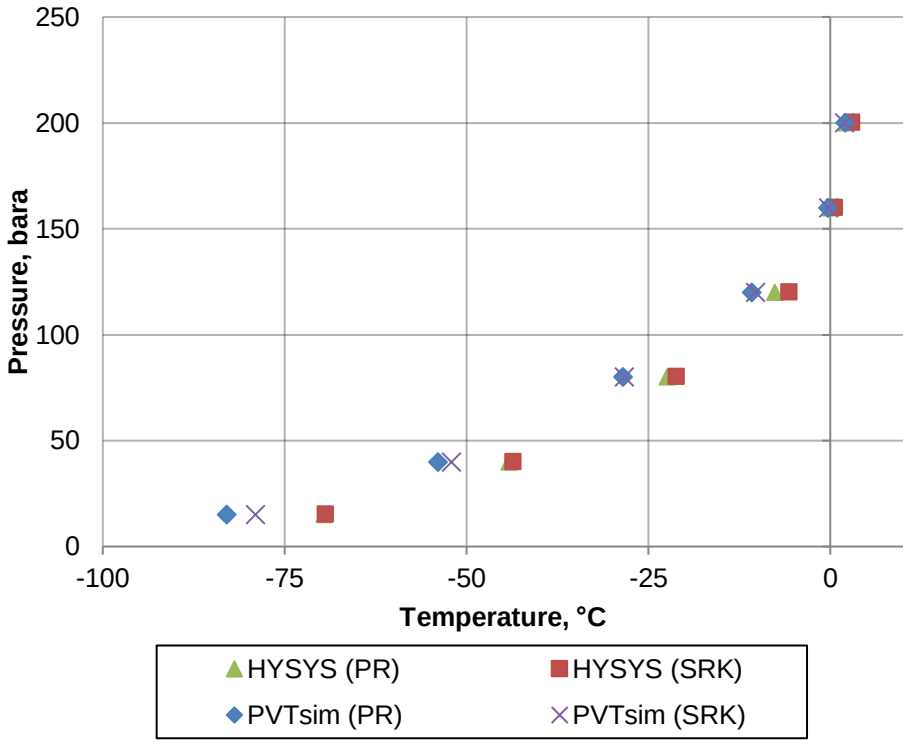

Fig.17 – Software Hydrate Equilibrium Data for Nitrogen

The variation in the predicted hydrate conditions vary to different extents for pure methane, carbon-dioxide and nitrogen. There is very little disagreement between the model used and the software for methane; almost 100% agreement across the full range of pressures. This is mostly true for pure nitrogen or carbon dioxide of which demonstrate only small deviations with the exception of the HYSYS SRK model, which showed significant deviation. However, research into each program's documentation revealed that they use the same variation of each EOS (**Table 2**) and solve them analytically by default.

Table 2 – PVTsim and HYSYS EOS Calculation Parameters

	Peng – Robinson	**Soave – Redlich – Kwong**
Critical Values	*The Properties of Gases and Liquids* (Reid et al. 1977)	
Equation of State	$P = \frac{RT}{V - b} - \frac{a(T)}{V(V + b) + b(V - b)}$	$P = \frac{RT}{V - b} - \frac{a(T)}{V(V + b)}$

	$Z^3 - (1 - B)Z^2 + (A - 2B - 3B^2)Z - (AB - B^2 - B^3) = 0$	$Z^3 - Z^2 + (A - B - B^2)Z - AB = 0$
A	$\frac{aP}{(RT)^2}$	$\frac{aP}{(RT)^2}$
B	$\frac{bP}{RT}$	$\frac{bP}{RT}$
a_i	$a_{ci}\alpha_i$	$a_{ci}\alpha_i$
a_{ci}	$0.45724\frac{R^2T_{ci}^2}{P_{ci}}$	$0.42748\frac{R^2T_{ci}^2}{P_{ci}}$
α_i	$\left[1 + m\left(1 - \left(\frac{T}{T_{ci}}\right)^{0.5}\right)\right]^2$	$\left[1 + m\left(1 - \left(\frac{T}{T_{ci}}\right)^{0.5}\right)\right]^2$
a	$\sum_{i=1}^{n}\sum_{i=j}^{n} x_i x_j (a_i a_j)^{0.5}(1 - k_{ij})$	$\sum_{i=1}^{n}\sum_{i=j}^{n} x_i x_j (a_i a_j)^{0.5}(1 - k_{ij})$
m_i	$0.37464 + 1.54226\omega_i - 0.269922\omega_i^2$	$0.480 + 1.547\omega_i - 0.176\omega_i^2$
m_i (if $\omega_i \leq 0.49$)	$0.37464 + \omega_i(1.48503\omega_i - 0.164423\omega_i + 0.01666\omega_i^2)$	-
ω_i	$-\log_{10}P_{ri}^{Sat}$ at $T_{ri}=0.7$	$-\log_{10}P_{ri}^{Sat}$ at $T_{ri} = 0.7$
b_i	$0.07780\frac{RT_{ci}}{P_{ci}}$	$0.08664\frac{RT_{ci}}{P_{ci}}$

The identical methods shared between PVTsim and HYSYS imply that the EOS is not likely a major source of discrepancy in the calculation of the hydrate equilibrium conditions. This was tested by generating critical PVT data with each EOS for binary mixtures of methane and nitrogen/carbon-dioxide. Data was generated for the critical pressure (P_c), critical temperature (T_c), critical molar volume ($\overline{V}_c$) and critical compressibility (Z_c). There were no discernible differences in this data between HYSYS and PVTsim; a sample of this data is listed in **Table 3**.

Table 3 – PVTsim and HYSYS Critical Property Calculations

	Peng – Robinson				Soave – Redlich – Kwong			
Critical Property	0.9 CH_4 - 0.1 CO_2		0.9 CH_4 - 0.1 N_2		0.9 CH_4 - 0.1 CO_2		0.9 CH_4 - 0.1 N_2	
	HSYS	PVTsim	HSYS	PVTsim	HSYS	PVTsim	HSYS	PVTsim
P_c, bara	53.85	52.48	48.69	48.23	54.16	52.69	48.6	48.21
T_c, °C	-70.25	-71.55	-87.52	-87.58	-69.76	-71.23	-87.4	-87.45
$\bar{V}_c$, cm^3/mol	95.65	97.53	100.3	101.23	103.9	106.0	109.2	110.5
Z_c	0.3053	0.3054	0.3166	0.3164	0.3328	0.3326	0.3435	0.3436

With little variation between their respective PVT models, the calculation method of the hydrate equilibrium properties must be different or use different reference values. The general methods associated with most hydrate equilibrium calculations are centred on the difference between the chemical potential of water in the hydrate state (μ^H) and the pure water state (μ^α),

$$\mu^H - \mu^\alpha = (\mu^H - \mu^\beta) + (\mu^\beta - \mu^\alpha). \quad \text{Eq. 4}$$

The $\mu^H - \mu^\beta$ term is the change in chemical potential of water from an empty lattice (β) to a gas stabilized lattice (H) and $\mu^\beta - \mu^\alpha$ represents the change in chemical potential from a pure water state (α) to an empty hydrate lattice. HYSYS and PVTsim solve **Eq. 4** by using their own model based on the fundamental statistical thermodynamic equation developed by van der Waals and Platteeuw (1959). The method in HYSYS uses an improved version to incorporate modifications by Parrish and Prausnitz (1972) which was shown to improve the predictability of the dissociation line in aqueous environments. The improvements of Ng and Robinson (1976, 1977) which provided better predictability of the Kihara parameters enabling better predictability in mixtures as well as aqueous systems is also incorporated. Calculation of the Langmuir adsorption coefficient is based on a complex approach by Ballard (2002). This approach proved to provide more accurate adsorption constants due to a multilayered cage approximation. HYSYS combines these modifications in the formulation of its own model, although the result of these modifications into a unified model is not directly specified in the program. It is also unclear what source the program uses for reference parameters associated with the transition from α to β. These reference parameters include the chemical potential ($\Delta\mu_0$), the change in molar volume (ΔV_0), and the change in molar

enthalpy, (ΔH_0). Reference data for these parameters in PVTsim is acquired from Erickson (1983) and Rasmussen and Pederson (2002). The overall approach in PVTsim is similar to HYSYS but one primary difference is the calculation of the Langmuir constant. PVTsim uses a simpler temperature dependent model from Munck et al. (1988) whom provided accurate Langmuir parameters in calculation of the temperature dependent model. Due the probability of a particular molecule occupying a particular hydrate cavity depending on the Langmuir constant for that unique occurrence, a noticeable difference in the hydrate equilibrium conditions predictions between HYSYS and PVTsim is not unlikely. This has been observed in this study and is summarized through **Fig.11** – **Fig.14**.

4.5 Empirical Relation

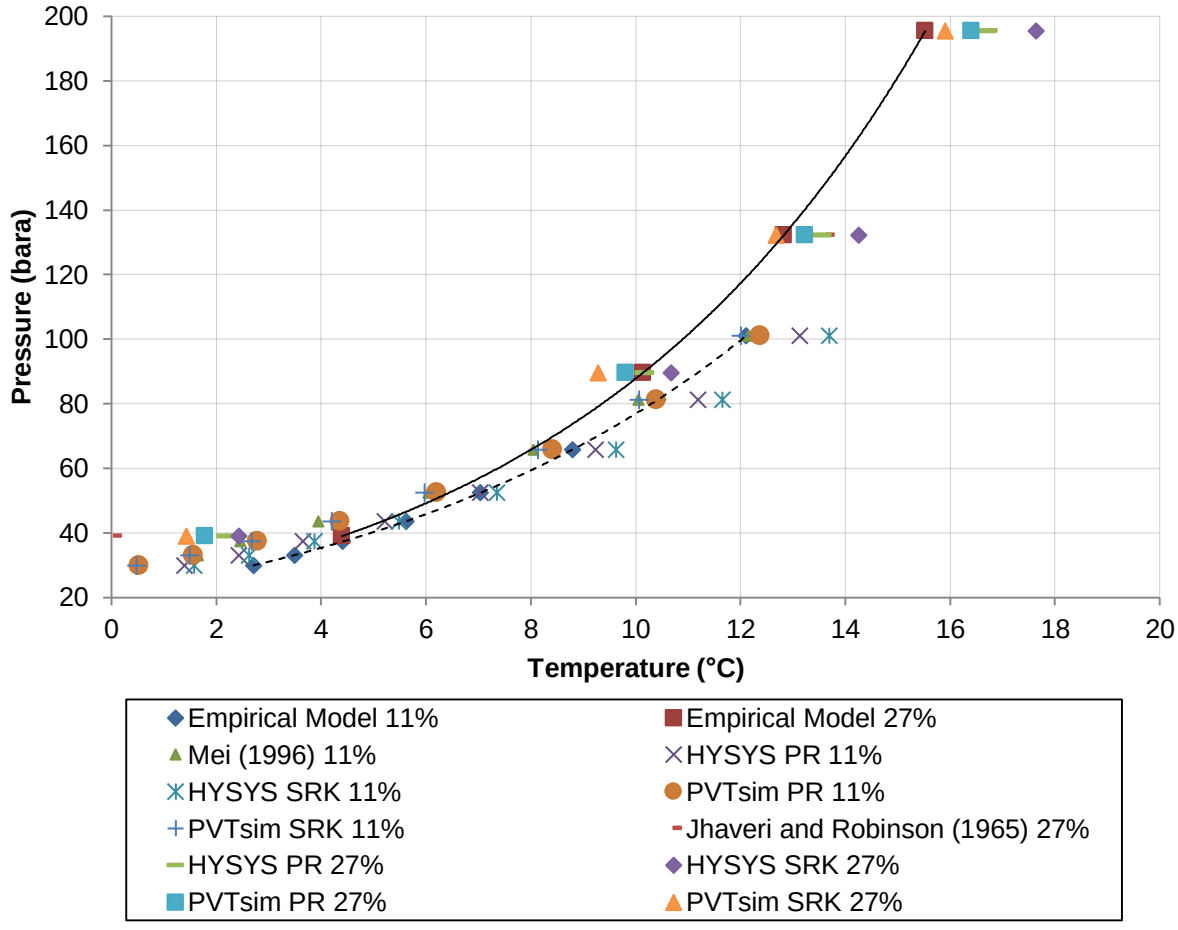

Fig.18 – Methane – Nitrogen Hydrate Equilibrium Data; Solid Line and dashed lines represent 11% and 27% model data respectively

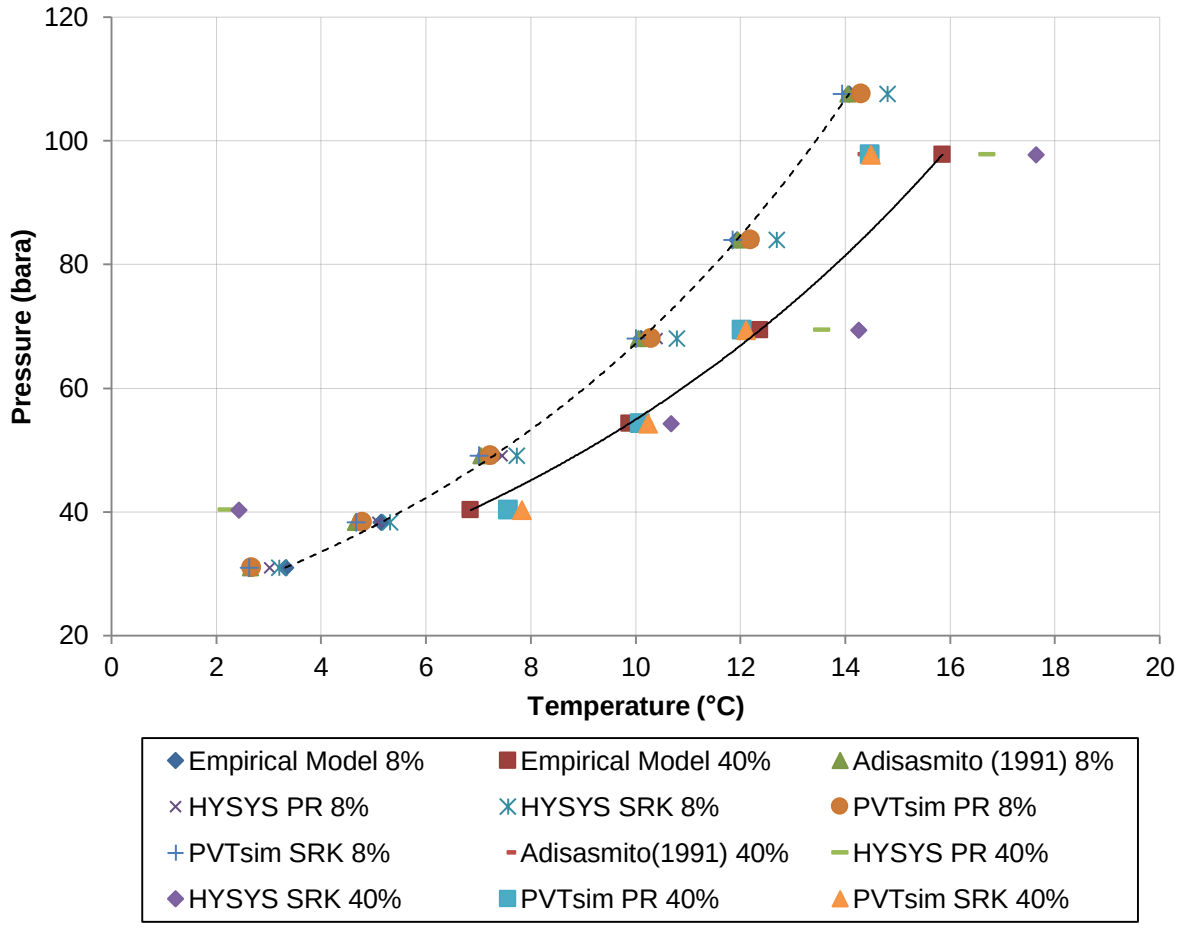

Fig.19 – Methane – Carbon-dioxide Hydrate Equilibrium Data; Solid Line and dashed lines represent 8% and 40% model data respectively

Substituting the values for the integrals and empirical constants into Eq. 1 then simplifying yields,

$$T_d(P,x_{N2},x_{CO2}) = 8.264\ln(P/21.31) - 5.05\ln(P/25.24)x_{N2} + 4.71\ln(P/17.34)x_{CO2} \quad \text{. . . . . Eq. 5}$$

The relationship expressed in **Eq. 5** allows the calculation of the dissociation temperature of a methane-based gas containing either or both nitrogen and carbon dioxide with a mole fraction of x_{N2} and x_{CO2} respectively. Deriving the constant for nitrogen resulted in a negative value, confirming that the introduction of nitrogen reduced the dissociation temperature. The opposite occurred for carbon dioxide; a positive value was determined, which is attributable to its hydrate stabilizing effect (Christiansen and Sloan 1994). The relation is reliable in the ranges of 40-180 bara and within the composition ranges tested. Inaccurate results were given when applying the model too far outside these ranges. This is expected because the model has essentially averaged the promotion and dilution effects of carbon-dioxide and nitrogen over the experimented pressure range. Therefore it less reliable

at the extremes of this range. Using Eq. 5, hydrate equilibrium data is generated using a range of pressures and compositions. The model is tested in regions outside of the range of tested conditions which the model was founded on in order to formally visualize any points of weakness. This is portrayed to be the case in the results illustrated in **Fig.18** and **Fig.19.**

5.0 Conclusion and Recommendations

An empirical model has been derived based solely on experimental data and incorporates the influences of nitrogen and carbon dioxide on their introduction to methane gas. The purpose of generating a model is to accurately calculate the dissociation temperature of a particular methane gas mixture diluted with nitrogen, carbon dioxide or both with any particular composition within range of those tested. It complements the experimental data and conveniently describes these results mathematically. Multiple examples reveal that the model is reliable based on comparison to the computed values generated by software capable of hydrate temperature prediction. However when applied outside the recommended ranges it became less reliable. The examples detailed in this paper deviate no more than 10% than those predicted and were often in the vicinity of 2-5% in the optimal working range, confirming the reliability of the experimental data and the empirical relation. The raw data also showed consistency with the temperatures computed via hydrate software, particularly at higher pressures where PVTsim excelled, usually differing by only 1-4%. Clausius – Clapeyron plots confirmed that sI hydrates formed in all experiments with methane-nitrogen and methane-carbon-dioxide gases. Slopes ranged from -8900 to -11100 which are consistent with literature values. The formation temperature was found to consistently occur at approximately 2-4 °C lower than the dissociation temperature; statistical measures confirmed that the dissociation temperature measurements are more precise and are reflective of the equilibrium temperature. The non-stoichiometric and random nature about gas hydrates and their formation are attributable to inconsistencies with expected trends with composition as well as the ability of hydrates to form despite cavities being absent of stabilizing guest molecules.

From a hydrate perspective, it is ideal that carbon dioxide is removed from production and processing streamsearly in the natural gas recovery and refinement process.This provides more leeway for processing conditions downstream on account of carbon dioxide’s ability to promote hydrate forming conditions and its increasing stabilizing effect at higher pressures. It would be beneficial to preserve and recycle any nitrogen recovered because of its ability to suppress hydrate formation and dissociation conditions by dilution. Alternatively, nitrogen can be introduced from an external source such as air where it may be considered as a

replacement to common hydrate inhibitors.This would be particularly cost-saving when operating conditions are known to be sitting on the verge of the hydrate zone as opposed to inside where nitrogen can be introduced instead of conventional inhibitors to decrease the likelihood of hydrate formation.

Acknowledgements

We'd like to acknowledge Shell Australia for their critical and financial support throughout the course of this project. Their direction, enthusiasm and encouragement towards this research is highly valued which has made this project possible.

References

Adisasmito, S, R. J Frank, and E. D Sloan. "Hydrates of Carbon Dioxide and Methane Mixtures." *Journal of Chemical Engineering Data 36 (1)*, 1991: 68-71.

Bai, Yong, and Qiang Bai. *Subsea Pipelines and Risers.* Elsevier, 2005.

Ballard, A. L, and E.D Sloan. "The Next Generation of Hydrate Prediction: I. Hydrate Standard States and Incorporation of Spectroscopy." *Fluid Phase Equilibria 194-197*, 2002: 371-383.

Buffet, Bruce A. "Clathrate Hydrates." *Annual Review of Earth and Planetary Science, Volume 28*, 2000: 477-509.

Carrol, John. *Natural Gas Hydrates: A Guide for Engineers.* Elsevier Science & Technology Books, 2002.

Christiansen, Richard L., and E. Dendy Sloan. "Mechanisms and Kinetics of Hydrate Formation." *Annals New York Academy of Sciences*, 1994: 283-305.

Dai, Sheng, Joo Yong Lee, and J. Carlos Santamarina. "Hydrate Nucleation in Quiscent and Dynamic Conditions." *Fluid Phase Equilibria Vol. 378*, 2014: 107-112.

Erickson, DD. *Development of a Natural Gas Hydrate Prediction Computer Program.* M.Sc. Thesis, Colorado School of Mines, 1983.

Herri, J. M, A Bouchemoua, M Kwaterski, A Fezoua, Y Ouabbas, and A Cameirao. "Gas Hydrate Equilibria for CO2-N2 and CO2-CH4 Gas Mixtures - Experimental Studies and Thermodynamic Modelling." *Fluid Phase Equilibria, Vol. 301 (2)*, 2011: 171-190.

Hobbs, P. V. *Ice Physics.* Oxford: Clarendon Press, 1974.

Jhaveri, J, and D. B Robinson. "Hydrates in the Methane-Nitrogen System." *The Canadian Journal of Chemical Engineering, 43*, 1965: 75-78.

Juan, Yu-Wan, Muoi Tang, Li-Jen Chen, Shaing-Lin Lin, Po-Chun Chen, and Yang-Ping Chen. “Measurements for the Equilibrium Conditions of Methane Hydrate in the Presence of Cyclopentanone or 4-Hydroxy-4-methyl-2-pentanone Additives.” *Fluid Phase Equilibria, Vol 386*, 2015: 162-167.

Kashchiev, Dimo, and Abbas Firoozabadi. “Nucleation of Natural Gas Hydrates.” *Journal of Crystal Growth*, 2002: 476-489.

Lederhos, J. P, L Christiansen, and E. D Sloan. “A First Order Method of Hydrate Equilibrium Estimation and its Use With New Structures.” *Fluid Phase Equilibria*, 1993: 83-445.

Max, Michael D., Arthur H. Johnson, and William P. Dillon. *Economic Geology of Natural Gas Hydrate, Volume 9.* Springer, 2006.

Mori, Yasukiko H. “Clathrate Hydrate Formation at the Interface Between Liquid CO2 and Water Phases - A Review of Rival Models Characterizing "Hydrate Films".” *Energy Conservation and Management*, 1998: 1537-1557.

Munck, Jan, Steen Skjold-Jorgensen, and Peter Rasmussen. “Computations of the Formation of Gas Hydrates.” *Chemical Engineering Science Vol. 43*, 1988: 2661-2672.

Ng, Heng-Joo, and Donald B. Robinson. “The Measurement and Prediction of Hydrate Formation in Liquid Hydrocarbon-Water Systems.” *AIChE Vol. 15*, 1976: 293-298.

Ng, Heng-Joo, and Donald B. Robinson. “The Prediction of Hydrate Formation in Condensed Systems.” *AIChE Journal Vol. 23*, 1977: 477-482.

Ota, M, and Y Qi. “Numerical Simulation of Nucleation Process of Clathrate Hydrates.” *JSME Int. J. Series B, 43*, 2000: 719-726.

Parrish, William R., and John M. Prausnitz. “Dissociation of Gas Hydrates Formed by Gas Mixtures.” *Ind. Eng. Chem. Process Des. Develop. Vol 11*, 1972: 26-35.

Rasmussen, C.P, and K.S Pederson. “Challenges in Modeling of Gas Hydrate Phase Equilibria.” *4th International Conference on Gas Hydrates.* Yokohama: Calsep, 2002.

Reid, Robert C, J. M Prausnitz, and Thomas K Sherwood. *The Properties of Gases and Liquids.* Mcgraw-Hill, 1977.

Schicks, J. M. “Natural Gas Hydrates.” *Handbook of Hydrocarbon and Lipid Microbiology*, 2010: 67-77.

Shin, Hyung Joon, Yun-Je Lee, Jun-Hyuck Im, Kyu Won Han, Jon-Won Lee, and Yongjae Lee. “Thermodynamic stability, spectroscopic identification and cage occupation of binary CO2 Clathrate Hydrates.” *Chemical Engineering Science*, 2009: 5125-5130.

Sloan, E. D, and F Fleyfel. “Hydrate Dissociation Enthalpy and Guest Size.” *Fluid Phase Equilibria*, 1992: 123-140.

Sloan, E. Dendy. *Clathrate of Natural Gas Hydrates, Third Edition.* Taylor & Francis Grou, 2008.

"The Prediction of Hydrate Formation in Condensed Systems." *AIChE*, 1977: 477-482.

Tohidi, B., R.W. Burgrass, A. Danesh, K.K. Ostergaard, and A.C. Todd. "Improving the Accuracy of Gas Hydrate Dissociation Point Measurements." *Annals New York Academy of Sciences*, 2000: 924-931.

Van der Waals, J.H, and J.C Platteeuw. "Clathrate Solutions." *Advances in Chemical Physics Vol. 2*, 1959: 59-85.

ZareNezhad, Bahman, Mona Mottahedin, and Farshad Varaminian. "A New Approach for Determination of Single Gas Hydrate Formation Kinetics in the Absence or Presence of Kinetic Promoters." *Chemical Engineering Science, Vol. 137*, 2015: 447-457.